Stoichiometric Excess of H_2O_2 as strategy of oxidant dosing for intensifying both Degradation and Mineralization of the Hydrochlorothiazide via UVC-H_2O_2, Dark-Fenton, and Photo-Fenton

Fernando J. V. Cunha-Filho,[1] Andressa Mota-Lima,[2] Claudio A. Oller do Nascimento,[3]

Osvaldo Chiavone-Filho, [1*]

1 Department of Chemical Engineering, Federal University of Rio Grande do Norte (UFRN), Av. Sen. Salgado Filho 3000, Natal-RN, Brazil

2 Department of Chemistry, Faculty of Philosophy, Sciences and Letters of Ribeirão Preto, University of São Paulo, Ribeirão Preto, São Paulo 14040-901, Brazil.

3 Departamento de Engenharia Química - Escola Politécnica, Universidade de São Paulo (USP), Cidade Universitária, São Paulo, 05508-900, SP, Brazil.

Corresponding author

Tel.: +55 16 98250 2311

Email address:

* osvaldo@eq.ufrn.br

Abstract. Hydrochlorothiazide (HCT) is a pharmaceutical micropollutant highly toxic to the environment, being strictly mandatory to oxidize it completely toward CO_2. In this context, how could the HCT oxidation via advanced oxidative processes benefit from the accelerated oxidation rates promoted by the mineralization stoichiometric excess of H_2O_2 ? Overall, this work elucidates the role of stoichiometric H_2O_2 concentration on promoting fast degradation/mineralization rates across Advanced Oxidative Processes (AOP). Employing 0.68 excess of H_2O_2, it was found absolute (100%) HCT degradation within 60 minutes and 95% within 30 min for UVC−H_2O_2 oxidation; however, the mineralization of HCT suffered limited optimization even at high H_2O_2 excess, being at the best performance 26.76% HCT mineralized via UVC photo-Fenton within 60 min at initial 2.00 H_2O_2 excess. Very presumably, the evaporation of H_2O_2 was the underlying reason for a low mineralization performance. Together with a detailed mathematical methodology, the time-synchronized evolution of both the residual H_2O_2 concentration and the TOC depletion were employed to infer the quantity of radical •OH that effectively was consumed by the micropollutant mineralization. The global mean efficiency of radicals •OH consumption by the HCT mineralization laid around 15% for UVC Fenton considering H_2O_2 excess of 2.00. Under these conditions, the residual H_2O_2 concentration depletes significantly within 30 minutes of UVC photo-Fenton oxidation, which indicates that either the solution heating or stirring is very likely to promote a substantial loss of H_2O_2 by evaporation in the beaker-assembled reactor.

Key-words. Accelerated degradation, Hydrochlorothiazide, H_2O_2 dosing method, Time-resolved H_2O_2 concentrations, H_2O_2-excess, Beaker-assembled Reactor.

1. Introduction

Hydrochlorothiazide (HCT) is a pharmaceutical micropollutant recently detected in the aquatic body employed to supply water to the city of Natal, northwest Brazil. Having in mind that the fragments of the HCT are toxic to the fauna and the unknown impact of human consumption of small doses of HCT via either drinkable water or cooked foods, it is urgent to find an efficient process to mineralize HCT at the largest degree as possible. Advanced oxidative processes (AOPs) [1-5] are suitable for attaining effective oxidation of HCT. Among the AOPs currently tested for oxidizing HCT, it is found processes like UV−H_2O_2 [6, 7], UV/$K_2S_2O_8$ [7], ozonation [8-10], photo-(electro)catalytic oxidation [11], electro-oxidation [12] and also the unusual H_2O_2 chemical oxidation in subcritical water [13]. All of them are capable to fully degrade HCT but rarely mineralize it. Except by the oxidation under the conditions of subcritical water [13], to which 85.22% HCT mineralization within 147 minutes was found; however, the authors used [13], according to our calculations, an astonishingly high excess of stoichiometric concentrations of H_2O_2, around 17,620 excess for mineralization. Furthermore, it was recently observed a fast HCT degradation rate with UV−H_2O_2 [7] that, according to our calculations, was achieved with an H_2O_2 excess of 0.215 for mineralization. The control of the oxidation performance with the initial stoichiometric concentration of H_2O_2 excesses for mineralization has mostly been unnoted. In this contribution, we disclose the importance of the initial H_2O_2 excesses for obtaining an outperformed oxidation.

The central aim of an AOP is the complete oxidation of the micropollutant, which secures the quality of water either for human consumption or for discharge with minimized risk of environmental impact. The complete oxidation of a micropollutant occurs when it is converted

exclusively into inorganic compounds such as inorganic acids, carbon dioxide, and water. However, it is far more common the occurrence of incomplete oxidation under relevant scaled-up/industrial conditions. In this case, among the final products are organic fragments of the original micropollutant, which may exhibit toxicity even higher than the original micropollutant. Below, the balanced equations for the complete and incomplete oxidation reaction of HCT ($C_7H_8N_3ClO_4S_2$) is respectively displayed

$$C_7H_8N_3ClO_4S_2 + 27\ H_2O_2 \rightarrow 7\ CO_2 + HCl + 3\ HNO_3 + 2\ H_2SO_4 + 27\ H_2O \quad (1)$$

$$C_7H_8N_3ClO_4S_2 + x\ H_2O_2 \rightarrow organic\ fragments, \text{ where } x \geq ½\ . \quad (2)$$

The complete oxidation of the micropollutant is a multistep reaction, meaning that the oxidation mechanism for the global reaction shown in equation 1 includes several step reactions such as the early steps of the incomplete oxidation shown in equation 2. Among the HCT fragments already detected were those expected for the earliest stages of oxidation, which has modifications to the functional groups coupled to either aromatic ring or the five-carbon ring [7, 8]. For this earliest stage, the stoichiometric quantity of the oxidant needed for incomplete oxidation represents just half of the micropollutant stoichiometric quantity. In other words, the ratio [*HCT]* to [H_2O_2] is 2 to 1. On the other hand, if considered a more advanced stage of the incomplete oxidation, other sorts of fragments may be found. Regarding the latest stage on the incomplete oxidation, organic acids of short-chair such as maleic acid,[14] oxalic acid,[15], and formic acid [16] have been identified for micropollutants in general. For this case, the stoichiometric oxidant quantity needed is far higher than half of that micropollutant quantity.

The experimental method employed to quantify the extension of the oxidation reaction leads to different concepts distinguishing micropollutant mineralization from micropollutant degradation. In principle, the extension of the oxidation may be followed by quantifying any

final product over time. According to the complete oxidation reaction in equations 1, such as the strong inorganic acids formed, i.e. cloridric acid (HCl), nitric acid (HNO_3) and sulfuric acid (H_2SO_4). However, these species can not strictly be followed for technical reasons. Recently, Garcia-Segura et al. [17] demonstrated the formation of volatile NOx during oxidation by •OH of N-containing aromatic pollutants. So, not all pollutant N-centers are converted into HNO_3 , which would bring inaccuracy on the measure of the extend of reaction by accessing the time-resolved concentration of HNO_3 experimentally. Further, anions as Cl^- and $SO_4{}^{2-}$can engage with side-reaction with the radical •OH , and its by-products could further reacts with H_2O_2.[18] In conclusion, the same inaccuracy could be found with them. The standard experimental method employed is the total organic content (TOC), and the amount of formed CO_2 is inferred by the TOC abatement over time. In this case, the extension of reaction is said to be mineralization. So, it is employed an indirect quantification of carbon dioxide (CO_2). Conceptually, mineralization quantifies the extension of the complete oxidation seen in equation 1. Alternatively, the extension of reaction could be inferred by measuring the temporal concentration of the reactants, either the micropollutant or the hydrogen peroxide (H_2O_2); however the time-resolved evolution of the H_2O_2 concentrations bring imprecision given that H_2O_2 is consumed by several side-reactions inherently present in liquid water. So as standard, the micropollutant concentrations is followed over time by means of analytical methods such as chromatography. The extension of reaction measured according this procedure leads to a different concept named degradation. In summary, the micropollutant mineralization conceptually is the extent of the reaction for the complete oxidation seen in equation 1, while the micropollutant degradation measures the earliest extend of oxidation reaction or the very earliest step reaction seen in equation 2.

Often, the degree of mineralizations and degradations are delayed. Such delay is closely related to how the concentration of the OH radical ($\cdot OH$) evolves during the oxidation evolution. The photolysis of H_2O_2 generates radicals $\cdot OH$

$$H_2O_2 \xrightarrow{h\nu} 2\,\cdot OH, \qquad (3)$$

that is the active oxidative agent intermediating both the mineralization reaction

$$C_7H_8N_3ClO_4S_2 + 54\,\cdot OH \rightarrow 7\,CO_2 + HCl + 3\,HNO_3 + 2\,H_2SO_4 + 27\,H_2O, \qquad (4)$$

and the degradation reaction

$$C_7H_8N_3ClO_4S_2 + \cdot OH \xrightarrow{k\sim10^9} organic\ fragment\ . \qquad (5)$$

The temporal evolutions of the $\cdot OH$ concentration determine either the rate or the extent of reactions 4 and 5. Given the larger stoichiometry of the $\cdot OH$ for the mineralization in comparison to the degradation, the degradation degree is always larger than the mineralization degree. Or yet, the complete or absolute degradation antecedes the absolute mineralization. Exceptionally distinct from this general role, recent findings showed the synchrony between absolute degradation and mineralization via photo-Fenton for a model micropollutant, the Acetyl Salicylic Acid, when manipulating the initial concentration of H_2O_2 [19]. Also, it indicated that the initial concentration of H_2O_2 calibrates the quantity of $\cdot OH$ that effectively engages with the micropollutant oxidation, which was found to be around 33% for the photo-Fenton [19].

In this contribution, we aim to evaluate the possibility to calibrate the local production of $\cdot OH$ by H_2O_2 scission and to verify the possibility to maximize the mineralization of a toxic and recalcitrant micropollutant, like the hydrochlorothiazide (HCT), by making use of the excesses of the H_2O_2 concentration for the stoichiometric mineralization reaction.

2. Methods

2.1 Materials

The set of experiments employed (99% Custódia Ltda), hydrogen peroxide (30 wt.%, Synth), and ferrous sulfate heptahydrate (99%, Neon). Standard HCT (Synth) were employed to prepare the solution with varied concentration of HCT, to correlate the HPLC peak with the concentrations of HCT, which in turn allowed to have a standard calibration curve used to estimate HCT concentration on the samples treated with AOP. For the vanadate method, it was used the metavanadate of ammonium (NH_4VO_3 from Alphatec). An inhibitor solution for the Fenton-based reactions, the one added right after sampling to stop the oxidation progress with the remaining reagents, was prepared using potassium iodide (0.1 M, 99%, Vetec), sodium sulfate (0.1 M, 99% Vetec) and sodium hydroxide (0.1 M; Vetec). All the experiments employed bi-distilled water (TE 1782, Tecnal, Brazil).

2.1 Beaker-assembled reactor

This work employed a simple unit for water treatment. Figure 1 drafts the details. A two-liter beaker of borosilicate glass was used to hold 1.5 L of HCT-containing water solution. The beaker was placed on the magnetic stirrer. A stir magnetic bar inside the beaker promoted the homogenization along the photo-processes. All the setup was assembled inside of a wooden box with inner walls reverted with aluminum foil in a manner to expose the foil bright side. A bulb-free high-pressure lamp of Mercury vapor (OSRAM E40 400W Hpl 400) fixed inside the box on the top wall, in a manner to irradiate all the solution from the top. The lamp of Mercury vapor features 45% of UVC radiation intensity. Such a box was maintained closed along with the

experiments, being the samples collected by a short polypropylene micro-pipeline connecting the beaker bottom to the external side of the box through a tiny hole on the lateral box wall. The samples were collected by a syringe plugged to the outside tail of the micro-pipeline.

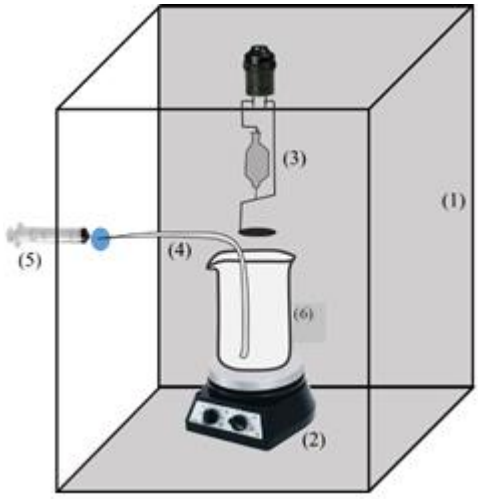

Figure 1. Scheme of the beaker reactor unit, which includes (1) a wooden box with inner walls reverted with aluminum paper in a manner to expose its bright side and externally measuring around 40×40×80 centimeters, inside which are located all other parts including (2) a magnetic stirrer, (3) bulb-free lamp of Mercury vapor, (4) polypropylene micro-pipeline for sampling, (5) a syringe for collecting samples, and (6) a beaker.

2.2 Batch experiments

All the experiments were carried without temperature control. For the kinetics experiments using Dark-Fenton, the reaction vessel was let inside of the wooden box with a turned-off lamp to prevent it from exterior light. For all the experiments, aliquots of 20 mL were taken at different time intervals, filtered through 0.45 μm Millipore filter, and analyzed for TOC and HCT

concentration. The sampling was carried out while the oxidation developed with a closed wooden box through the micro-pipeline connecting the solution at the bottom of the beaker with a syringe plugged to the outside micro-pipeline tail.

2.3 Chemical Analysis

The TOC concentration was measured by a TOC analysis (TOC-V 5000A, Shimadzu, Japan). The concentration of Hydrochlorothiazide was measured by HPLC (Proeminence HPLC-DAD, Shimadzu, Japan) using C18 Varian (150mm×4.6 mm, 5 μm particle size) column. The HPLC is equipped with a degasifier (DGU-20As), ternary pump (LC-20AT), automatic sampling (SIL-20A HT), furnace (CTO-20A), photodiode array detector (SPD-M20A), detector UV set at 294 nm, and data acquisition interface (CBM-20A). The mobile phase used as eluent was a mixture of water plus acetonitrile (70:30, v/v) at a flow rate of 1.0 mL min^{-1}. The chromatographic conditions just described allows for a separation of the baseline within only eight minutes. Before TOC and HPLC analysis, the samples were filtered employing a filter Millipore 0.45 μm.

This work employs the vanadate method [20, 21] to quantify the residual peroxide in the samples. Several details were already described in previous work.[19] In summary, metavanadate of ammonium is added into the sample, the metavanadate anion then reacts with the residual peroxide forming a red-orange color peroxovanadium cation (VO_2^{+3}), which in turn could be detected and quantified by 450 nm absorption. Spectroscopic determinations were performed using a UV-Visible Spectrophotometer (Varian-Cary) and 1 cm cells of quartz. The solution of metavanadate (0.062 M) and H_2SO_4 (0.58 M) was prepared by slowly adding 15 ml of concentrated sulfuric acid (Aldrich) into a solution of the metavanadate of ammonium under

magnetic stirring and heating (~ 40 °C) until complete dissolution. After cooling down, the solution was diluted in ultrapure water to reach 500 mL of a volumetric balloon.

2. Results and Discussions

The onset for developing a process capable of absolute mineralization is the calculation of the needed quantity of oxidant for the complete oxidation of the micropollutant considering the concentration in question. If otherwise, the oxidation will be incomplete, and so the mineralization degree will attain the lowest/mildest values because of a mere absence of oxidant. In the present study, we established 20.84 and 70.00 $mg \cdot L^{-1}$ or equivalently 0.070 and 0.238 $mmol \cdot L^{-1}$ as initial concentration of HCT, which corresponds to 5.90 and 20.00 $mg \cdot L^{-1}$ of total organic carbon, respectively. According to the stoichiometric relation between HCT and the oxidant in reaction 1, each HCT molecule requires 27-times more molecules of oxidant. So, the mineralization for the aforementioned micropollutant concentrations require 1.89 and 6.43 $mmol \cdot L^{-1}$ of H_2O_2, respectively. Table 1 summarize all this information. The degree of mineralization will be studied in terms of the needed stoichiometric quantity of H_2O_2 for reaction 1. Eventually, we will compare the degree of degradation in terms of the stoichiometric related to reaction 3, to which each HCT molecule relates to one radical $\cdot OH$, in turn, half H_2O_2 molecule. We recall the parameter named stoichiometric excess of H_2O_2, which was already defined elsewhere as [19]

$$Excess = \frac{[H_2O_2]_{Local}}{[H_2O_2]_{ST}}, \quad (6)$$

being $[H_2O_2]_{Local}$ the H_2O_2 concentration in the micropollutant-containing solution and the $[H_2O_2]_{ST}$ being the stoichiometry concentration of H_2O_2 for a complete oxidation reaction.

$[H_2O_2]_{Local}$ stands for the local value at either the oxidation onset or at any time along with the oxidation. For an excess equal one, there is sufficient oxidant for absolute mineralization, i.e. complete oxidation of micropollutant toward the CO_2. For an excess lower than one, the micropollutant may suffer a complete degree of degradation but not of mineralization for mere oxidant starvation. For an excess higher than one, there is an excess of oxidant in comparison to the micropollutant which not necessary would lead to absolute mineralization but, instead, has potential to that. Given that the fact that radical $^{\bullet}OH$ engages with several side-reactions, it is very important to understand the efficiency with which $^{\bullet}OH$ effectively reacts with the micropollutant. In this context, the excess of oxidant is mandatory for attaining absolute mineralization.

Table 1: Summary of the stoichiometric concentrations of H_2O_2, $[H_2O_2]_{ST}$, for both complete and incomplete oxidation considering two different HCT concentrations.

Initial concentration of HCT (ppm / mg · L^{-1} /mM)	$[H_2O_2]_{ST}$ Mineralization	$[H_2O_2]_{ST}$ Degradation
0.070 mmol · L^{-1} 20.84 mg · L^{-1} (TOC = 5.9 ppm)	1.89 mmol · L^{-1}	0.035 mmol · L^{-1}
0.238 mmol · L^{-1} 70.00 mg · L^{-1} (TOC = 20 ppm)	6.43 mmol · L^{-1}	0.119 mmol · L^{-1}

3.1 Relating the stoichiometric excess of H_2O_2 with the initial dosage of H_2O_2 during UVC−H_2O_2 oxidation

Figure 2 shows how different initial doses of H_2O_2, which is added all at once on the onset of the experiment, into the solution of 0.070 $mmol \cdot L^{-1}$ HCT affects the kinetic of HCT degradation over 60 minutes during UVC-H_2O_2 oxidation. The experiments started with different initial excess of H_2O_2. Overall, the results show that absolute degradation is reached within 50 minutes regardless of the initial concentration. Besides, two major aspects are noted for the initial excess of H_2O_2. First, even a fraction of H_2O_2 excess leads to complete degradation, as is the case seen for 0.68 excess. Second, excessively large excesses of H_2O_2 adds no benefit for the degradation rate as was the case for 4.76 excess, or even worst there is a delay on the depletion over time as was the case for 6.80 excess. Those aspects are discussed below in terms of what $^{\bullet}OH$ concentrations are expected for them to explain their kinetic behaviors.

The fact of the 0.68 excess to be capable of attaining complete degradation is not a surprise. The excess throughout this work is measured regarding the complete oxidation seen in reaction 1 and not regarding the incomplete oxidation seen in reaction 2. For incomplete oxidation, the stoichiometry between HCT and H_2O_2 follows the reaction 3, meaning that each HCT molecule to be degraded needs one radical $^{\bullet}OH$, which in turn relates with half molecule of H_2O_2, at the least. The 0.68 excess represents 1.286 $mmol \cdot L^{-1}$ H_2O_2, leading to excess for degradation around 36.74 (1.286 $mmol \cdot L^{-1}$ ÷ 0.035 $mmol \cdot L^{-1}$). Table 2 summarizes H_2O_2 excesses for either mineralization or degradation considering all data in figure 2. This value of 36.74 excess for degradation is substantially high and justifies the little enhancement observed on the degradation degrees when employing the H_2O_2 excesses for mineralization larger than 0.68; for instance, 85% degradation is observed for 0.68 excess at 20 minutes, and little improvement beyond this value is seen for 2.04 and 3.40 excesses. This conjecture however

modifies for excesses above 3.40 seen on the plate at right, to which either no improvement on the degradation passes to be seen with 4.76 excess or even contrarily, a delayed degradation degree is seen with 6.80 excess.

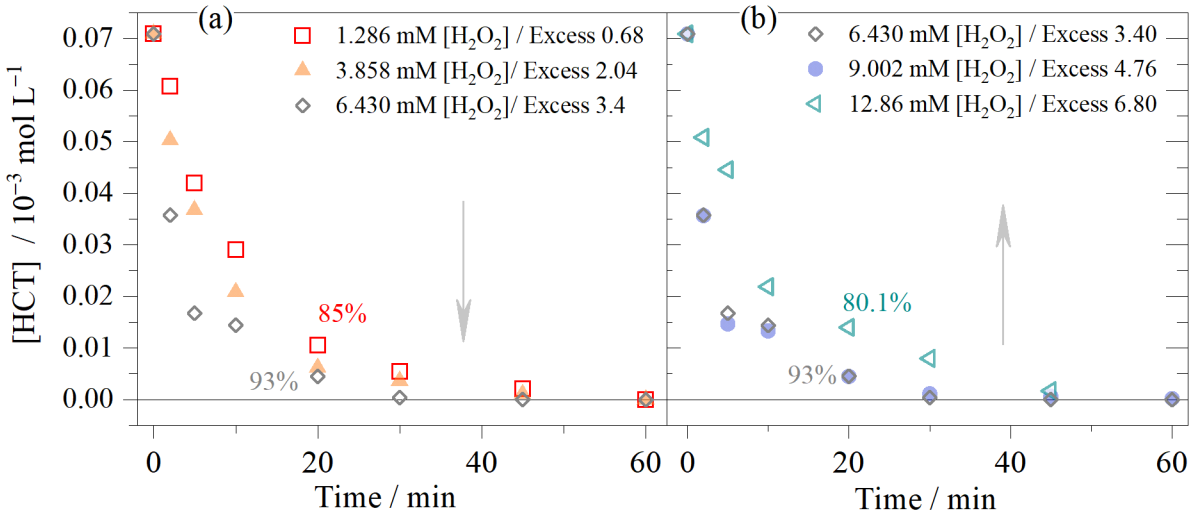

Figure 2. Kinetic decay of HCT concentration during oxidation via UVC-H_2O_2 when considering different initial concentrations of H_2O_2, $[H_2O_2]_0$. The stoichiometric H_2O_2 for mineralization is 1.89 mmol·L^{-1}, being the excess find by the ratio $[H_2O_2]_0$ to $[H_2O_2]_{ST}$. The excesses shown in the legend refers to the absolute mineralization.

The 6.80 excess for mineralization shown in figure 2 represents 12.86 mmol · L^{-1} H_2O_2, actually leading to excess for degradation around 367 (12.86 mmol · L^{-1}/0.035 mmol · L^{-1}). This value is excessively high. Considering that the micropollutant-containing solution from this work has a very well-controlled composition, it is possible to sort out the following radiation reaction out of the radiolysis data set [22] as the most prominent candidate to explain the results in figure 2 for high excess of H_2O_2,

$$H_2O_2 + {}^{\bullet}OH \xrightarrow{k \sim 10^7} O_2^{\bullet -} + H_2O. \quad (7)$$

In reaction 7, H_2O_2 is consumed by ${}^{\bullet}OH$, meaning that the H_2O_2 passes to compete with the HCT by the ${}^{\bullet}OH$ locally available. At substantially high excesses of H_2O_2, the rate of reaction 5 and 7 reaches almost similar order of magnitude as we detailed below

$$v_7 = 10^7\ [H_2O_2][{}^{\bullet}OH] = 10^7 \times 12.86\ 10^{-3}[{}^{\bullet}OH] = 12.86\ 10^4[{}^{\bullet}OH]$$

$$v_5 = 10^9[HCT][{}^{\bullet}OH] = 10^9 \times 0.070\ 10^{-3}[{}^{\bullet}OH] = 7\ 10^4[{}^{\bullet}OH].$$

This way, the effective consumption of the ${}^{\bullet}OH$ by HCT via reaction 5 expectedly decreases, in turn justifying the mild delay seen in figure 2 for the degradation degree observed for excesses of 3.4 and 6.8, which were 93.0% and 80.1% respectively at the time of 20 minutes.

3.2 Relating the stoichiometric excess of H_2O_2 with the initial dosage of H_2O_2 during Dark-Fenton and UVC−Fenton oxidation

Figure 3 shows the TOC depletion employing Dark-Fenton to oxidize a 0.238 mmol·L^{-1} HCT solution. Table 3 assist to find out the H_2O_2 excess regarding mineralization used in figure 3, which was H_2O_2 excess of 0.2 and 2.0. In agreement with the expectations, the experiment for 0.2 excess suffers negligible mineralization, around 1% at 60 minutes because of the mere lack of oxidant. This result typifies the cases where the limited mineralization occurs due to H_2O_2 starvation. Contrariwise, for 2.0 excess of H_2O_2 for mineralization, the TOC abates till 5.51% within 60 minutes, which is significantly low. As Dark-Fenton accounts exclusively on the Fe^{+2} catalyst to promote the H_2O_2 conversion into radicals OH, we could conclude that, given results in figure 3, there are limited temporal productions of radicals by the Dark-Fenton mechanism.

And such ineffectiveness demonstrated not to be overcome by using twice large stoichiometry of H_2O_2. How would this conjecture modify in presence of UVC radiation?

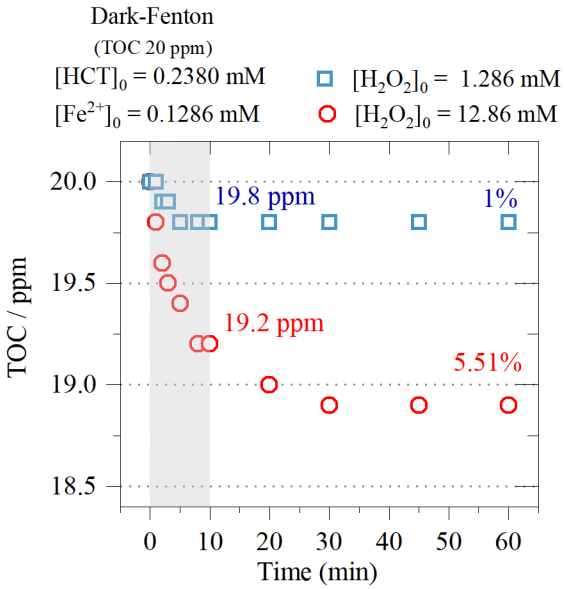

Figure 3. The TOC depletion when oxidizing 0.238 mmol·L^{-1} HCT solution with Dark-Fenton with distinct excesses of H_2O_2. The experiments were carried out inside the reactor box with a closed door and a turned-off lamp. It was used 0.1286 mmol·L^{-1} of Fe^{+2} as the catalyst.

Figure 4 shows how different initial excesses of H_2O_2 impact both the degradation and mineralization when oxidizing 0.238 mmol·L^{-1} HCT via UVC photo-Fenton. The differentiation between H_2O_2 excesses for degradation and mineralization is again explicitly shown in table 3, which assists to interpret the results in figure 4. Globally, all the initial excesses of H_2O_2 leads to an absolute degradation within one hour of photo-Fenton oxidation, except by the initial concentration of 0.62 mmol·L^{-1}, to which only 10.5% degradation was observed after one hour. According to table 3, 0.62 mmol·L^{-1} refers to 5.21 excess of H_2O_2 for degradation, which is substantially inferior to that 36.74 excess for degradation (0.68 excess of mineralization) used in figure 2, to which 100% mineralization were attained within one hour of UVC−H_2O_2. This

astoundingly different results for degradation only highlights the crucial role of the H_2O_2 excesses for attaining accelerated degradation rate across different AOP.

Table 2: Summary of the H_2O_2 excesses for both complete and incomplete oxidation considering the concentration of H_2O_2 and HCT in figure 2.

Initial concentration of H_2O_2	H_2O_2 excess	
	Mineralization	Degradation
1.286 mmol · L^{-1}	0.68	36.74
3.858 mmol · L^{-1}	2.04	110.23
6.430 mmol · L^{-1}	3.40	183.71
9.002 mmol · L^{-1}	4.76	257.20
12.86 mmol · L^{-1}	6.80	367.43
Initial HCT concentration of 0.070 mmol · L^{-1}		
$[H_2O_2]_{ST}$ for Mineralization is 1.89 mmol · L^{-1}		
$[H_2O_2]_{ST}$ for Degradation is 0.035 mmol · L^{-1}		

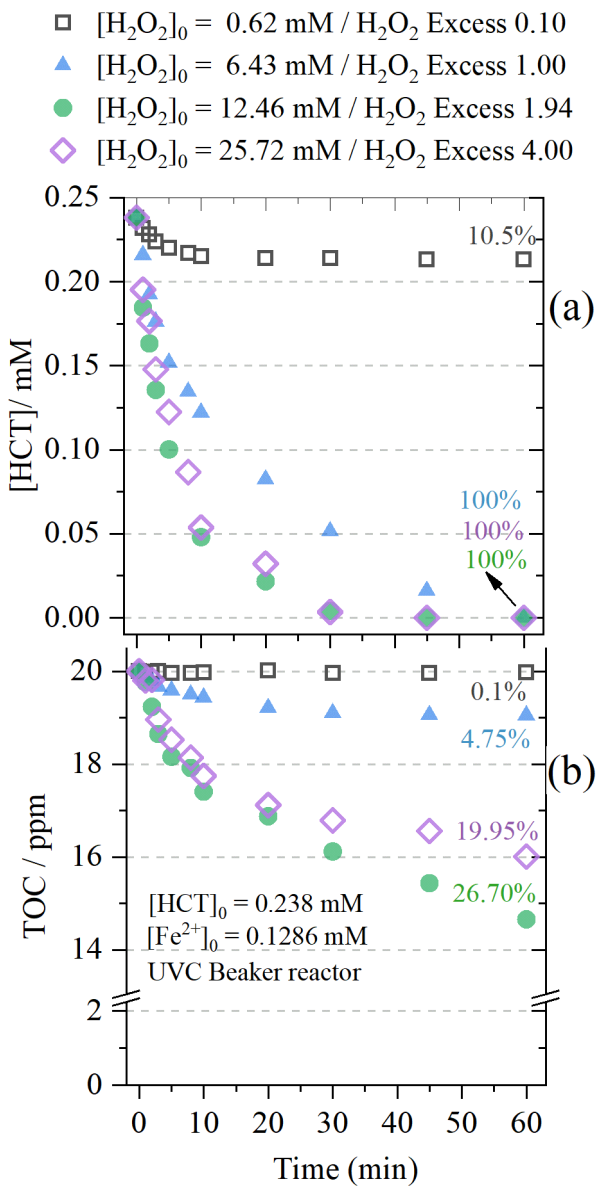

Figure 4. Impact of the initial concentration of H_2O_2 on the photo-Fenton oxidation of 20 ppm (0.238 mmol·L^{-1}) Hydrochlorothiazide (HCT) measured in terms of the time-resolved (a) HCT concentration and (b) total organic carbon. It was used the beaker-assembled reactor equipped with a UVC lamp and 0.1286 mmol·L^{-1} of Fe^{+2} catalyst. Percentages written next to the symbols represent the degree of abatement on the HCT concentration and the total organic carbon (TOC). The excesses shown in the legend refers to the absolute mineralization.

Figure 4 on the plate (b) shows the mineralization for the photo-Fenton oxidation when the H_2O_2 excesses for mineralization from 0.1 to 4.0 are employed as the initial condition. When the oxidation onset has 0.1 excess for oxidation the negligible 0.1% of mineralization degree is reached, just as expected given that only 10 % of the oxidant agent required for the complete oxidation was indeed present. The next three excesses reveal interesting aspects of the oxidation time evolution. What to expect if the initial concentration of H_2O_2 were strictly that exact amount for complete mineralization? According to figure 4, the excess 1.0 exhibit very limited 4.75% mineralization within 60 minutes, despite the absolute degradation had been reached within this period, in turn elucidating that HCT no longer exists but one of its very earliest aromatic-ring-containing fragments given that 4.75% mineralization relates to less than one carbon center converted to CO_2 per HTC molecule. What to expect for excesses larger than one? According to figure 4, all of them reach absolute degradation within 30 minutes, whereas 60 minutes is required to reach 36.70 and 19.95% mineralization for excesses of 1.94 and 4.00, respectively. The inefficient consumption of H_2O_2 by the HCT oxidation justifies the need for an oxidant agent excess. Both 1.94 and 4.00 excesses seemed insufficient as only very mild mineralization were reached, in turn, make us wonder whether better performances would be attained with larger excesses; but, it would be not. The delayed mineralization from excess 1.94 to 4.00 indicates an already larger excess as very presumably the reaction 7 is substantially fired for the 4.00excess.

Table 3: Summary of the H_2O_2 excesses for both complete and incomplete oxidation considering the concentration of H_2O_2 and HCT from figure 4.

Initial concentration of H_2O_2	H_2O_2 excess	
	Mineralization	Degradation
0.62 mmol · L^{-1}	0.10	5.21
1.286 mmol · L^{-1}	0.20	10.81
6.43 mmol · L^{-1}	1.00	54.03
12.43 mmol · L^{-1}	1.94	104.45
12.86 mmol · L^{-1}	2.00	108.07
25.72 mmol · L^{-1}	4.00	216.13
Initial HCT concentration of 0.238 mmol · L^{-1}		
$[H_2O_2]_{ST}$ for Mineralization is 6.43 mmol · L^{-1}		
$[H_2O_2]_{ST}$ for Degradation is 0.119 mmol · L^{-1}		

3.4 Efficiency of •OH scavenger by the micropollutant at a high H_2O_2 excess for Photo-Fenton oxidations

In the previous sections, the excess of H_2O_2 was manipulated by the initial dose of H_2O_2; however, to obtain a time-resolved curve for the H_2O_2 excesses along with the oxidation evolution, it is strictly necessary to have the time-synchronized assessment of both the TOC and residual concentration of H_2O_2. For this reason, the H_2O_2 concentrations were measured via the spectroscopic vanadate method using half of the aliquot collected for TOC. The second reason for measuring the time-resolved evolution of the H_2O_2 concentrations is our aim to estimate instantaneous variation on both the TOC and H_2O_2 concentrations and, therefore, to evaluate how

many of the H_2O_2 molar quantity was effectively consumed by the HCT mineralization over the instantaneous interval. Later in this section, instantaneous rates will be employed to discuss the efficiency of •OH scavenger by the micropollutant.

Figure 5 shows the synchronized time-evolution of both TOC and H_2O_2 concentrations for the photo-Fenton oxidation. These results allowed us to infer the efficiency with which the radical •OH is consumed by the HCT oxidation reaction. The rationalization starts by first considering that for a given time interval, Δt, a given variation on the H_2O_2 concentrations is observed on the depletion curve for the residual H_2O_2, $\Delta[H_2O_2]_{Local}$. In practical terms, the value for $\Delta[H_2O_2]_{Local}$ is obtaining with the time-resolved H_2O_2 depletion curves seen on the plate (a) figures 5. Additionally, we rationalize the term $\Delta[H_2O_2]_{ST}$ by defining it as the variation on the H_2O_2 concentration related to the HCT mineralization according to the stoichiometry seen in reaction 1. So, rationalization made, we can define the efficiency of the radical •OH consumption by HCT oxidation as a function of the time intervals Δt by the ratio

$$f(\Delta t) \equiv \frac{\Delta[H_2O_2]_{ST}}{\Delta[H_2O_2]_{Local}} \times 100\,. \qquad (8)$$

To conclude the rationalization, we decipher a practical manner to have experimental access to the value of $\Delta[H_2O_2]_{ST}$. The TOC depletion curves being converted to a degree of mineralization by dividing the TOC variation (ΔTOC) over a given time interval by the initial TOC value (TOC_0). The equivalent value of HCT concentration effectively mineralize is found by multiplying the remaining degree of mineralization by $[HCT]_0$, the initial HCT concentration. According to the stoichiometry of reaction 1, each molar concentration of depleted HCT is related to a 27-times larger molar concentration of depleted H_2O_2. With all these considerations, the term $\Delta[H_2O_2]_{ST}$ is defined as

$$\Delta[H_2O_2]_{ST} \equiv 27 \times \left(\frac{\Delta TOC}{TOC_0}\right) \times [HCT]_0 . \quad (9)$$

Combining equations 8 and 9, the efficiency of the radical •OH consumed by the HCT oxidation can be found

$$f(\Delta t) = \frac{\Delta TOC}{TOC_0} \times \frac{[HCT]_0}{\Delta[H_2O_2]_{Local}} \times 2700 . \quad (10)$$

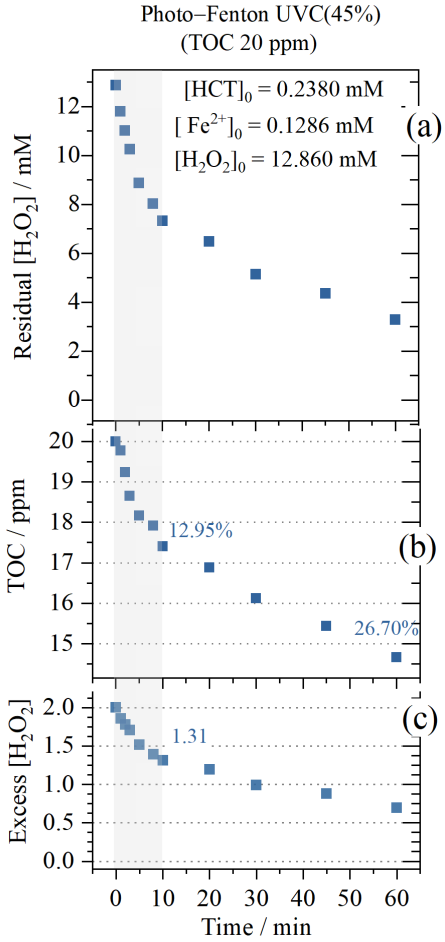

Figure 5. Synchronized time-evolution of (a) the residual concentrations of H_2O_2, (b) the TOC, and (c) the time-resolved excess of H_2O_2, when oxidizing 0.238 mmol·L^{-1} HCT solution in presence of 0.1286 mmol·L^{-1} Fe^{+2} as the catalyst. The photo-Fenton were carried out inside the reactor box with a closed door and turned-on lamp. It was used 2.0 H_2O_2 excesses for the mineralization.

Figure 6 shows the efficiencies of radical •OH consumption by the HCT oxidation for two sorts of time intervals. Mean average efficiency is obtained for any interval between the oxidation onset (time zero) and the updated time, as indicated by the horizontal lines in plate b. If otherwise, the interval includes two immediate consecutive experimental points, the efficiency reflects that interval, which is so-called instantaneous efficiency and it is indicated by the vertical lines in the plate c.

On average, the photo-Fenton reached an efficiency of ~15 %, a mark that is substantially inefficient in comparison to the approximately 33% of efficiency obtained with the tubular reactor for the oxidation of Acetyl Salicylic Acid [19]. Attribute the inefficiency to differences on the micropollutant molecular structure is insufficient to formulate a complete justification. Considering the beaker-assembled rector setup from this work, chances are that substantial quantity of H_2O_2 is lost by evaporation during the HCT oxidation for several reasons: (a) the stirring with open beaker favor H_2O_2 evaporation, (b) the absence of any strategy of heat dissipation make impossible to formulate a justification to any rise on the temperature; the first author maintained the wooden box close during all the 60 minutes long, which prevented the first author to note the temperature raise, and the enhanced temperature does favor H_2O_2 evaporation. We are aware that the residual concentration of H_2O_2 shown in Figures 4 and 5 carries a contribution due to the evaporation that was intrinsic to the reactor setup. Yet, we cannot discharge/deny the generality of the effects caused by the stoichiometric excess of H_2O_2 on the degradation and mineralization observed across different AOP employed in this work. Or finally, we can not hide from the audience the importance of an example of how not to set a reactor.

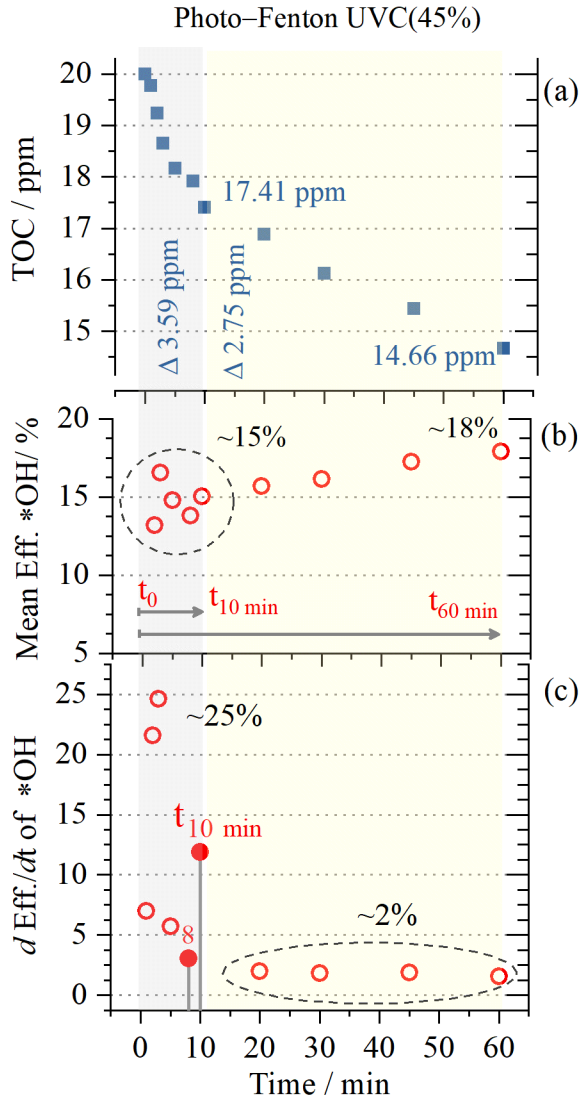

Figure 6. Efficiency to which the radical □OH is scavenged by the HCT oxidation is estimated for average and instantaneous time intervals. The efficiency was obtained using the data shown in figure 5 and equation 10. Plate (a) shows the TOC to facilitate the interpretation.

Despite all the likelihood of H_2O_2 evaporation to induce an underestimation of the H_2O_2 consumption by the HCT mineralization, we can not deny the conspicuous importance of the results in relative terms. For instance, ~15 % efficiency of radical •OH scavenger by HCT,

despite the underestimated value, it has consistency with the low TOC abatements seen in figure 5. Besides, other comparisons are safely possible. Because of reaction 7, it is possible to infer that both the efficiency of H_2O_2/•OH consumption and the instantaneous concentration of the radical •OH is lower for Dark-Fenton in comparison to the Photo-Fenton. Considering the rate of reaction 7, the only presumable explanation would be a concentration of radical •OH lower for Dark-Fenton than for Photo-Fenton. Note below how the rate of reactions 4 and 7 are written for initial HCT concentration of 0.238 mmol·L^{-1}

$$v_7 = 10^7\ [H_2O_2][\cdot OH] = 10^7 \times 12.86\ 10^{-3}[\cdot OH] = 12.86\ 10^4[\cdot OH]\ ,$$

$$v_4 = 10^9[HCT][\cdot OH]^{>1} = 10^9 \times 0.238\ 10^{-3}[\cdot OH]^{>1} = 23.80\ 10^4[\cdot OH]^{>1}.$$

The condition $v_7 = v_4$ happens, only if the value of $[\cdot OH]$ were around 1.0 mmol·L^{-1}; if otherwise, they were tenths below 1.0 mmol·L^{-1}, the rate of reaction would be $v_7 > v_4$. The first condition depicts the scenario for Photo-Fenton, whereas the second describes the kinetics for the Dark-Fenton.

Outlook

In the Prof. Chiavone-Filho and Prof. Nascimento research groups, several homogenous photo-chemical reactors [23-26] have been tested over the years, and for none of the cases, the stoichiometric excess of H_2O_2 was pointed out categorially. Even though dating back to the outstanding fast mineralization earliest obtained by Silva et al. [23], the signals of the role played by the H_2O_2 excess were hidden there, but the H_2O_2 excess had remained unnoted by Silva et al. mainly because of the method used for H_2O_2 dose, which in the case was the continuous H_2O_2 supply from a concentrated stock solution. For H_2O_2 dose method based on stationary flow, the

H_2O_2 excess must be rationalized in terms of the stationary excess within the reactive zone, which can be calibrated by both (a) the H_2O_2 concentration in the stock solution and the stationary steady flow of either (b) the H_2O_2–rich or (c) pollutant–rich solutions. There are uncountable manners to design a flow reactor for this aim. For all of them, all those three reactor parameters aforementioned need to be balanced to control the stationary H_2O_2 excess within the reactive zone. The recently developed reactor by Villar et al. [27] features a radial addition of H_2O_2 into streaming of pollutant-rich solution, and presumably, the advance from this work certainly will benefit the development of that creative reactor by offering guide on how the stationary H_2O_2 concentration inside the reactive zone must be to attain outperformed rates of mineralization. At last but not least, the stoichiometric excesses of oxidant agent, despite studied here for the H_2O_2, must not be limited to solely H_2O_2, but rather be extended to other sources of radical-initiated oxidation such as the activated persulfate-like oxidative agent [28].

Conclusion

In this contribution, the residual concentration of hydrogen peroxide (H_2O_2) is measured in synchrony with the TOC depletion during oxidation of hydrochlorothiazide (HCT) via AOPs, aiming to understand the stoichiometric time evolution related to the target oxidation reaction, the HCT mineralization or reaction 1. Such recorded dynamics is employed to infer the efficiency with which the oxidant is consumed by the HCT oxidation reaction, one among several other side reactions that competitively scavenges the radical •OH. As the time variation of the content of CO_2, that is a product for the reaction 1, can be correlated with the stoichiometric variation of H_2O_2 concentration for the same reaction, the engagement of radical •OH with side reaction can be directly estimated by comparing such stoichiometric variation with the time variation of

H_2O_2 concentration recorded by the methavanadate method. A mathematical rationale for this analysis of efficiency of oxidant consumption by the mineralization reaction is presented, and it is used as methodology for calculating the efficiency of OH radical •OH consumption. At the best, such efficiency laid around 15% for the Photo-Fenton reaction, which is considered a low value that presumably is associated with an additional loss of H_2O_2 either by decomposition reaction or evaporation induced by both the lamp heat and stirring of the open reactor.

Acknowledgments

This work was sponsored by (i) the National Program for Academic Cooperation (PROCAD-88881.068433/2014-01), and (ii) Graduate Program in Chemical Engineering of the Federal University of Rio Grande do Norte (UFRN). Andressa M.L. gratefully acknowledges the individual financial support awarded by the National Council of Research and Development CNPq (#155046/2018-7) and CAPES (# 88887.198057/2018-00).

References

[1] S. Gligorovski, R. Strekowski, S. Barbati, D. Vione, Environmental Implications of Hydroxyl Radicals (•OH), Chemical Reviews, 115 (2015) 13051-13092.
[2] S. Wacławek, H.V. Lutze, K. Grübel, V.V.T. Padil, M. Černík, D.D. Dionysiou, Chemistry of persulfates in water and wastewater treatment: A review, Chemical Engineering Journal, 330 (2017) 44-62.
[3] C. von Sonntag, The basics of oxidants in water treatment. Part A: OH radical reactions, Water Science and Technology, 55 (2007) 19-23.
[4] E. Brillas, S. Garcia-Segura, Benchmarking recent advances and innovative technology approaches of Fenton, photo-Fenton, electro-Fenton, and related processes: A review on the relevance of phenol as model molecule, Separation and Purification Technology, 237 (2020) 116337.
[5] E. Brillas, I. Sirés, M.A. Oturan, Electro-Fenton Process and Related Electrochemical Technologies Based on Fenton's Reaction Chemistry, Chemical Reviews, 109 (2009) 6570-6631.
[6] C.E.S. Paniagua, I. Amildon Ricardo, E.O. Marson, B.R. Gonçalves, A.G. Trovó, Simultaneous degradation of the pharmaceuticals gemfibrozil, hydrochlorothiazide and

naproxen and toxicity changes during UV-C and UV-C/H2O2 processes in different aqueous matrixes, Journal of Environmental Chemical Engineering, 7 (2019) 103164.
[7] M. Fernández-Perales, M. Sánchez-Polo, M. Rozalen, M.V. López-Ramón, A.J. Mota, J. Rivera-Utrilla, Degradation of the diuretic hydrochlorothiazide by UV/Solar radiation assisted oxidation processes, Journal of environmental management, 257 (2020) 109973.
[8] E. Borowska, M. Bourgin, J. Hollender, C. Kienle, C.S. McArdell, U. von Gunten, Oxidation of cetirizine, fexofenadine and hydrochlorothiazide during ozonation: Kinetics and formation of transformation products, Water Research, 94 (2016) 350-362.
[9] F.J. Real, J.L. Acero, F.J. Benitez, G. Roldán, L.C. Fernández, Oxidation of hydrochlorothiazide by UV radiation, hydroxyl radicals and ozone: Kinetics and elimination from water systems, Chemical Engineering Journal, 160 (2010) 72-78.
[10] E.M. Rodríguez, G. Márquez, E.A. León, P.M. Álvarez, A.M. Amat, F.J. Beltrán, Mechanism considerations for photocatalytic oxidation, ozonation and photocatalytic ozonation of some pharmaceutical compounds in water, Journal of environmental management, 127 (2013) 114-124.
[11] P.J. Mafa, R. Patala, B.B. Mamba, D. Liu, J. Gui, A.T. Kuvarega, Plasmonic Ag3PO4/EG photoanode for visible light-driven photoelectrocatalytic degradation of diuretic drug, Chemical Engineering Journal, 393 (2020) 124804.
[12] N. Contreras, J. Vidal, C. Berríos, L. Villegas, R. Salazar, Degradation of Antihypertensive Hydrochlorothiazide in Water from Pharmaceutical Formulations by Electro-Oxidation Using a BDD Anode, Int. J. Electrochem. Sci., 10 (2015) 9269-9285.
[13] G.Ö. Yabalak E , Nural Y . , Mineralization of Hydrochlorothiazide using Hydrogen Peroxide in Subcritical Water. , Journal of the Turkish Chemical Society Section A: Chemistry., 5 (2018) 1135-1144.
[14] M.F. Murrieta, I. Sirés, E. Brillas, J.L. Nava, Mineralization of Acid Red 1 azo dye by solar photoelectro-Fenton-like process using electrogenerated HClO and photoregenerated Fe(II), Chemosphere, 246 (2020) 125697.
[15] S. Garcia-Segura, E. Brillas, L. Cornejo-Ponce, R. Salazar, Effect of the Fe3+/Cu2+ ratio on the removal of the recalcitrant oxalic and oxamic acids by electro-Fenton and solar photoelectro-Fenton, Solar Energy, 124 (2016) 242-253.
[16] Z. Ye, D.R.V. Guelfi, G. Álvarez, F. Alcaide, E. Brillas, I. Sirés, Enhanced electrocatalytic production of H2O2 at Co-based air-diffusion cathodes for the photoelectro-Fenton treatment of bronopol, Applied Catalysis B: Environmental, 247 (2019) 191-199.
[17] S. Garcia-Segura, E. Mostafa, H. Baltruschat, Could NOx be released during mineralization of pollutants containing nitrogen by hydroxyl radical? Ascertaining the release of N-volatile species, Applied Catalysis B: Environmental, 207 (2017) 376-384.
[18] F.C. Moreira, R.A.R. Boaventura, E. Brillas, V.J.P. Vilar, Electrochemical advanced oxidation processes: A review on their application to synthetic and real wastewaters, Applied Catalysis B: Environmental, 202 (2017) 217-261.
[19] F.J.V. Cunha-Filho, A. Mota-Lima, L.A. Ratkievicius, D.J. Silva, D.N. Silva, O. Chiavone-Filho, C.A. Oller do Nascimento, Rapid mineralization rate of acetylsalicylic acid in a tubular photochemical reactor: The role of the optimized excess of H2O2, Journal of Water Process Engineering, 31 (2019) 100856.
[20] R.F.P. Nogueira, M.C. Oliveira, W.C. Paterlini, Simple and fast spectrophotometric determination of H2O2 in photo-Fenton reactions using metavanadate, Talanta, 66 (2005) 86-91.

[21] M.C. Oliveira, R.F.P. Nogueira, J.A. Gomes Neto, W.F. Jardim, J.J.R. Rohwedder, Sistema de injeção em fluxo espectrofotométrico para monitorar peróxido de hidrogênio em processo de fotodegradação por reação foto-Fenton, Química Nova, 24 (2001) 188-190.
[22] G.V. Buxton, C.L. Greenstock, W.P. Helman, A.B. Ross, Critical Review of rate constants for reactions of hydrated electrons, hydrogen atoms and hydroxyl radicals (·OH/·O− in Aqueous Solution, J. Phys. Chem. Ref. Data, 17 (1988) 513-886.
[23] S.S. da Silva, O. Chiavone-Filho, E.L. de Barros Neto, A.L.N. Mota, E.L. Foletto, C.A.O. Nascimento, Photodegradation of non-ionic surfactant with different ethoxy groups in aqueous effluents by the photo-Fenton process, Environmental technology, 35 (2014) 1556-1564.
[24] A.J. Luna, C.A.O. Nascimento, E.L. Foletto, J.E.F. Moraes, O. Chiavone-Filho, Photo-Fenton degradation of phenol, 2,4-dichlorophenoxyacetic acid and 2,4-dichlorophenol mixture in saline solution using a falling-film solar reactor, Environmental technology, 35 (2013) 364-371.
[25] J.E.F. Moraes, F.H. Quina, C.A.O. Nascimento, D.N. Silva, O. Chiavone-Filho, Treatment of Saline Wastewater Contaminated with Hydrocarbons by the Photo-Fenton Process, Environmental Science & Technology, 38 (2004) 1183-1187.
[26] A.L.N. Mota, L.G.L. Neto, E.L. Foletto, O. Chiavone-Filho, C.A.O.d. Nascimento, Analysis of solar and artificial UVA irradiations on the photo-Fenton treatment of phenolic effluent and oilfield produced water, Chemical Engineering Communications, 205 (2018) 1594-1603.
[27] V.J.P. Vilar, P. Alfonso-Muniozguren, J.P. Monteiro, J. Lee, S.M. Miranda, R.A.R. Boaventura, Tube-in-tube membrane microreactor for photochemical UVC/H2O2 processes: A proof of concept, Chemical Engineering Journal, 379 (2020) 122341.
[28] X. Duan, S. Yang, S. Wacławek, G. Fang, R. Xiao, D.D. Dionysiou, Limitations and prospects of sulfate-radical based advanced oxidation processes, Journal of Environmental Chemical Engineering, 8 (2020) 103849.

Highlights

- ~ 85% HCT degradation within 20 minutes of UVC-H_2O_2;
- The •OH consumption by the pollutant oxidation was around 13% for photo-Fenton;
- H2O2 evaporation is the underlying reason for low efficiency of radical •OH consumption;

- The stoichiometric excess of [H_2O_2] modulates both the radicals •OH concentration and the efficiency of •OH scavenger by HCT.

Graphical abstract